

Performance Bounds for Near-Field Velocity Estimation with Modular Linear Array

Khalid A. Alshumayri, Mudassir Masood, *Senior Member, IEEE*, Ali A. Nasir, *Senior Member, IEEE*

Abstract—Velocity estimation is a cornerstone of the recently introduced near-field predictive beamforming. This paper derives the Cramér–Rao bounds (CRBs) for joint radial and transverse velocity estimation within a predictive beamforming framework employing a modular linear array (MLA). We obtain closed-form expressions that characterize the interplay between array geometry and estimation accuracy, showing that increasing the inter-module separation enlarges the effective aperture and reduces the transverse-velocity CRB, while the radial-velocity CRB remains largely insensitive to this separation. Furthermore, we show that an MLA can achieve the same accuracy as a collocated ULA with fewer antennas and quantify the relation between inter-module spacing and antenna savings. The derived expressions are validated through simulations by comparing them with the mean-squared error (MSE) of the maximum likelihood estimator (MLE) reported in the literature.

Index Terms—Near-field, integrated sensing and communications (ISAC), predictive beamforming, velocity estimation.

I. INTRODUCTION

THE adoption of large-aperture arrays has given rise to a near-field (NF) channel model that assumes a spherical rather than planar wavefront. This makes the NF channel jointly dependent on the propagation direction and distance. Moreover, the curvature of the spherical wavefront encodes both radial and transverse motion, enabling the estimation of both velocity components using a monostatic array. Based on these estimated velocities, the target's future direction and distance can be forecast. This is the key idea behind the predictive beamforming framework in [1], where a maximum likelihood estimator (MLE) is employed for NF velocity sensing without requiring pilot signals. However, this pioneering work did not investigate fundamental performance bounds for velocity estimation. Reference [2] derived the Cramér–Rao bounds (CRBs) for both radial and transverse velocities for single-input multiple-output (SIMO) monostatic radar which differs from the predictive-beamforming framework considered here.

Realizing beamforming with a large number of antennas poses significant challenges in both hardware and signal processing. To mitigate this issue, the modular linear array (MLA) architecture, consists of multiple collocated uniform linear array (ULA) modules, enable the construction of a larger effective aperture. As illustrated in Fig. 1, the modules are separated by inter-module spacing larger than the inter-element spacing, easing deployment on rooftops or building

Khalid A. Alshumayri is with the Department of Electrical Engineering, King Fahd University of Petroleum and Minerals, Dhahran 31261, Saudi Arabia.

Mudassir Masood and Ali A. Nasir are with the Electrical Engineering Department and the Interdisciplinary Research Center for Communication Systems and Sensing (IRC-CSS), King Fahd University of Petroleum and Minerals, Dhahran 31261, Saudi Arabia.

façades while extending the NF region [3]–[6]. Prior work on MLA has derived the CRBs for range and angle estimation [7], and the analysis was extended in [8] to MLA with non-uniform inter-module spacing. However, the CRBs for NF velocity estimation using MLAs have not been reported in the literature.

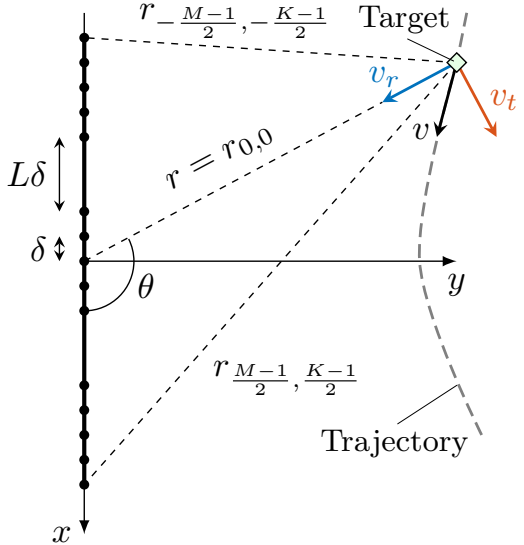


Fig. 1. Near-field velocity sensing employing modular linear array.

In this letter, we derive the performance bound for joint velocity estimation using MLA. The contributions of this work are: (i) We derive tractable CRB expressions for joint radial and transverse velocity estimation in the NF region, revealing explicit dependence on the parameters of MLA, and verify that the mean-squared error (MSE) of the MLE in [1] is efficient and attains the derived CRBs. (ii) We obtain a closed-form expression for the predictive-beamforming array gain under velocity mismatch due to estimation errors and show that transverse-velocity estimation error contribute more severely to performance degradation compared to radial-velocity counterparts. (iii) We establish a practical design rule: enlarging inter-module separation reduces the transverse-velocity CRB via effective-aperture growth, while the radial-velocity CRB remains essentially unchanged. This suggests that MLA architecture can achieve the same transverse-velocity estimation accuracy as a collocated ULA but with fewer antennas. In particular, we show that for MLA with inter-module separation equivalent to 25% of the aperture of collocated ULA, we can remove approximately 17% of the antennas in the ULA while achieving the same transverse-velocity CRB. However, the

cost of reducing the total number of antennas is a negligible increase in the radial-velocity CRB.

II. SIGNAL AND SYSTEM MODEL

As illustrated in Fig. 1, we consider a near-field communications system. The base station (BS) is equipped with a modular antenna array composed of K modules, each with M antennas, resulting in a total of MK antennas. The antenna spacing is uniform and denoted by δ . The modules are placed evenly along the x -axis with an inter-module spacing $L\delta$. The location of the m -th element in the k -th module is given by the vector $\mathbf{w}_{m,k} = [x_{m,k}, 0]^T$ where $m = 0, \pm 1, \dots, \pm \frac{M-1}{2}$, $k = 0, \pm 1, \dots, \pm \frac{K-1}{2}$. The coordinates are given by $x_{m,k} = (Uk + m)\delta$, where $U = M + L - 1$. Further, the same antenna array is employed for transmitting and receiving, made possible by circulators and full-duplex capability [9]. The (m, k) -th entry of the array response vector at time index n is given by [1], [10]

$$[\mathbf{a}_n(r, \theta, v_r, v_t)]_{m,k} = \exp \left\{ -j \frac{2\pi}{\lambda} (r_{m,k} + v_{m,k} nT_s) \right\}, \quad (1)$$

where $r_{m,k} = \sqrt{r^2 - 2r(Uk + m)\delta \cos \theta + (Uk + m)^2 \delta^2}$ is the distance between the target and the (m, k) -th antenna in module k , and T_s is the symbol duration. The Doppler shift is caused by $v_{m,k} = q_{m,k}v_r + p_{m,k}v_t$, where v_r and v_t denote the radial and transverse velocities of the target with respect to the origin, $q_{m,k}$ and $p_{m,k}$ denote the projection coefficients

$$q_{m,k} = \frac{r - (Uk + m)\delta \cos \theta}{r_{m,k}}, \quad p_{m,k} = \frac{(Uk + m)\delta \sin \theta}{r_{m,k}} \quad (2)$$

The coefficients satisfy $q_{m,k}^2 + p_{m,k}^2 = 1$, and if the FF model is used, such that $r_{m,k} \approx r - (Uk + m)\delta \cos \theta$, it will result in $q_{m,k} = 1$ and $p_{m,k} = 0$, which explains the reason the transverse velocity remains unobservable under that model. However, for the NF region, this approximation is no longer valid. In addition, we assume a point-like moving target. The target movement is confined within the radiating NF region, specifically at a distance greater than the Fresnel distance [11], which is defined as $d_F = 0.5\sqrt{A^3/\lambda}$ where $A = \delta[K(M-1) + L(K-1)]$ is the aperture length, which can equivalently be expressed as $A = \delta[U(K-1) + M-1]$.

For notation convenience, let ϕ represent the target parameters $\{r, \theta, v_r, v_t\}$. Assuming that the downlink channel between BS and target is dominated by the line-of-sight (LoS) component of the channel, the received baseband echo signal at the array, reflected by the moving target, at time index n for the l -th coherent processing interval (CPI) will be described as

$$\mathbf{y}_l(n) = \beta \mathbf{a}_n(\phi_l) \mathbf{a}_n^T(\phi_l) \mathbf{x}(n) + \mathbf{z}(n) \quad (3)$$

where $\beta \in \mathbb{C}$ represents the reflection coefficient that depends on both the round-trip pathloss and the radar cross section (RCS), $\mathbf{z}(n)$ is circular white Gaussian noise. The transmit signal $\mathbf{x}(n)$ is designed according to the estimated parameters ϕ from the previous CPI.

A. Predictive Beamforming

The advantages of employing predictive beamforming in designing the transmit signal $\mathbf{x}(t)$ are twofold: 1) Doppler compensation and, and 2) prediction of the target's future location by utilizing the kinematic model

$$\hat{r}_{l+1} = \hat{r}_l + \hat{v}_{r,l} NT_s, \quad \hat{\theta}_{l+1} = \hat{\theta}_l + \hat{v}_{t,l} NT_s / \hat{r}_l. \quad (4)$$

The predicted parameters ϕ are used to steer the beam in the next CPI. Accordingly, the transmit signal is designed as

$$\mathbf{x}(n) = \frac{\mathbf{a}_n^*(\hat{\phi}_l)}{\sqrt{MK}} s(n) \quad (5)$$

where $s(n)$ represents the information symbol that satisfy $|s(n)|^2 = 1$. A rough estimate of the parameters v_r and v_t can be obtained from the previous CPI and used in the current CPI to compensate for the Doppler shift and predict the target's future location [1]. Substituting (5) into (3), the received echo signal at the BS will be ¹

$$\mathbf{y}_l(n) = \beta \psi(n) \mathbf{a}_n(\phi_l) s(n) + \mathbf{z}(n), \quad (6)$$

where $\psi(n)$ is the array-gain function. It characterizes the array gain under velocity mismatch due to estimation error from the previous CPI

$$\psi(n) = \frac{1}{\sqrt{MK}} \sum_{m,k} e^{-j \frac{2\pi}{\lambda} (q_{m,k} \Delta_{v_r} + p_{m,k} \Delta_{v_t}) nT_s}, \quad (7)$$

where Δ_{v_r} and Δ_{v_t} denote the mismatches between the true and estimated radial and transverse velocities, respectively.

B. Array-Gain Function

To simplify $\psi(n)$, we adopt the approximation $q_{m,k} \approx 1$ and $p_{m,k} \approx \frac{(Uk + m)\delta \sin \theta}{r}$ [12],

$$\psi(n) \approx \frac{e^{-j \frac{2\pi}{\lambda} \Delta_{v_r} nT_s}}{\sqrt{MK}} \left(\sum_m e^{-j \tilde{\Delta}_{v_t} m} \right) \left(\sum_k e^{-j \tilde{\Delta}_{v_t} U k} \right), \quad (8)$$

where $\tilde{\Delta}_{v_t} = \frac{2\pi}{\lambda} \left(\frac{\delta \sin \theta}{r} \right) \Delta_{v_t} nT_s$. The summation can be recognized as a Dirichlet kernel function. Hence it directly follows that

$$\psi(n) = \frac{e^{-j \frac{2\pi}{\lambda} \Delta_{v_r} nT_s}}{\sqrt{MK}} \frac{\sin(M\tilde{\Delta}_{v_t}/2)}{\sin(\tilde{\Delta}_{v_t}/2)} \frac{\sin(KU\tilde{\Delta}_{v_t}/2)}{\sin(U\tilde{\Delta}_{v_t}/2)}. \quad (9)$$

Ideally, when $\hat{v}_r \approx v_r$ and $\hat{v}_t \approx v_t$, the array gain satisfies $\psi(n) \approx \sqrt{MK}$, which is numerically demonstrated in Section IV. Besides, applying the point scatterer model, the reflection coefficient can be expressed as [13], $|\beta|^2 = \frac{P_t G_t G_r \sigma_{RCS}}{(4\pi)^3 r^4}$, where P_t and σ_{RCS} represent the transmit power and the radar cross-section, respectively, while, G_t and G_r denote the antenna gains for transmitter and receiver respectively. For a monostatic setup, the antenna gains are equal, i.e., $G_r = G_t$.

¹A similar derivation applies to the uplink scenario. If the transmitted signal is known (e.g., a pilot), then $\mathbf{y}_l(n) = \beta \mathbf{a}_n(\phi_l) s(n)$.

III. CRBS FOR VELOCITY ESTIMATION

The CRB provides a theoretical lower limit on the variance of unbiased estimators of a deterministic parameter. It is derived from the Fisher Information, which quantifies the amount of information that an observable random variable carries about an unknown parameter. The Fisher information matrix (FIM) for radial and transverse velocity is given by

$$\mathbf{F} = \begin{bmatrix} J_{v_r v_r} & J_{v_r v_t} \\ J_{v_t v_r} & J_{v_t v_t} \end{bmatrix}.$$

Let the unknown parameters $\zeta = [v_r \ v_t]^T$, the FIM elements under the white Gaussian noise model can be found as [14, Ch. 15.7]

$$J_{ij} = \frac{2}{\sigma^2} \sum_n \sum_m \sum_k \Re \left\{ \frac{\partial \mathbf{u}^H(n)}{\partial \zeta_i} \frac{\partial \mathbf{u}(n)}{\partial \zeta_j} \right\},$$

where $\frac{\partial}{\partial \zeta} \mathbf{u}(n) = \beta \sqrt{MK} \frac{\partial}{\partial \zeta} \mathbf{a}_n(\phi) s(n)$ is the noise-free version of the received echo signal at the BS. Accordingly, the three FIM elements can be readily obtained $J_{v_r v_r} = \gamma MK \sum_{m,k} q_{m,k}^2$, $J_{v_t v_t} = \gamma MK \sum_{m,k} p_{m,k}^2$, and $J_{v_r v_t} = \gamma MK \sum_{m,k} q_{m,k} p_{m,k}$, where we define the SNR as

$$\gamma = \left(\frac{2\pi}{\lambda} \right)^2 \frac{|\beta|^2 N(N+1)(2N+1)}{3\sigma^2} T_s^2. \quad (10)$$

Then, the CRBs for radial and transverse velocities correspond to the diagonal elements of the inverse of the FIM.

$$\text{CRB}(v_r) = \frac{J_{v_r v_r}}{\text{Det } \mathbf{F}}, \quad \text{CRB}(v_t) = \frac{J_{v_t v_t}}{\text{Det } \mathbf{F}}. \quad (11)$$

To obtain more tractable CRB expressions, we employ a simple yet tight approximation. In particular, FIM can be simplified using the following theorem

Theorem 1: Consider a target located at a distance $r \geq d_F$, and assume that the aperture satisfies $U(K-1) + M - 1 \gg \lambda/\delta$. Then the following approximations hold:

$$\sum_{m,k} p_{m,k}^2 \approx \frac{MK}{12} (U^2(K^2-1) + (M^2-1)) \frac{\delta^2}{r^2} \sin^2 \theta, \quad (12)$$

$$\sum_{m,k} q_{m,k} p_{m,k} \approx \frac{MK}{12} (U^2(K^2-1) + (M^2-1)) \frac{\delta^2}{r^2} \cos \theta \sin \theta. \quad (13)$$

Proof: Please refer to Appendix A. ■

For a standard uniform linear array, $\lambda/\delta = 2$, hence the condition $U(K-1) + M - 1 \gg 2$ is typically satisfied. The expression (12) shows that the information on transverse velocity increases with the inter-module separation through the factor U^2 . Moreover, we can derive the closed-form CRBs as in the follow

$$\text{CRB}_{\text{Mod}}^{(v_r)} = \frac{12}{\gamma(MK)^2 \left(12 - \left(\frac{\delta}{r} \right)^2 (U^2(K^2-1) + M^2-1) \right)}, \quad (14)$$

$$\text{CRB}_{\text{Mod}}^{(v_t)} = \frac{12(r/\delta)^2}{\gamma(MK)^2 (U^2(K^2-1) + M^2-1) \sin^2 \theta}. \quad (15)$$

The existence of the CRBs is guaranteed when $\frac{12}{U^2(K^2-1) + M^2-1} > (\delta/r)^2$, which holds for $U(K-1) + M - 1 \gg \lambda/\delta$. Note that the radial CRB is approximately not dependent on the target angle because the projection component $q_{m,k}$ is insensitive to the target angle since the quantity $\delta/r_{m,k}$ is relatively small. Also, it is largely unaffected by the inter-module spacing owing to the small term $(\delta/r)^2$. However, increasing the inter-module spacing reduces the transverse CRB. Additionally, for the special case when $L = 1$ and $M_0 = MK$, the result is reduced to the CRB for the conventional ULA in [2]

$$\text{CRB}_{\text{ULA}}^{(v_r)} = \frac{12}{\gamma M_0^2 \left(12 - \left(\frac{\delta}{r} \right)^2 (M_0^2 - 1) \right)}, \quad (16)$$

$$\text{CRB}_{\text{ULA}}^{(v_t)} = \frac{12(r^2/\delta^2)}{\gamma M_0^2 (M_0^2 - 1) \sin^2 \theta}. \quad (17)$$

Proposition 1: Since $\delta/r \ll 1$, the radial CRB is much less than the transverse CRB, as confirmed numerically in Section IV. Because the increased inter-module spacing results in $\text{CRB}_{\text{Mod}}^{(v_t)} < \text{CRB}_{\text{ULA}}^{(v_t)}$, it is natural to ask whether we can save some antennas by widening the spacing while reducing the number of elements, so that the MLA transverse CRB matches the collocated ULA transverse CRB. We have shown through analysis below and later through numerical results that with an MLA having inter-module separation equivalent to 25% of the aperture of a collocated ULA, we can remove approximately 17% of the antennas in the ULA while achieving the same transverse-velocity CRB.

Proof: Formally, we seek parameters for which

$$\text{CRB}_{\text{ULA}}^{(v_t)} = \text{CRB}_{\text{Mod}}^{(v_t)}. \quad (18)$$

Concretely, for some choice of inter-module separation \bar{L} and number of antenna per-module \bar{M} satisfying $K\bar{M} < M_0$, the modular array's CRB will equal that of the ULA. To this end, the inter-module spacing is written in units of the reference ULA aperture, $\bar{L} = 1 + \eta(M_0 - 1)$, where the parameter η denotes the fraction of the ULA aperture added as extra spacing between adjacent modules. The minimum separation that achieves the same performance as ULA can be directly obtained from (18) and is given by

$$\eta = \frac{1}{M_0 - 1} \left(\sqrt{\frac{M_0^2(M_0^2 - 1) - (\bar{M}^2 - 1)(\bar{M}K)^2}{(K^2 - 1)(\bar{M}K)^2}} - \bar{M} \right). \quad (19)$$

The spacing η can be written in terms of the fraction of antennas used $h = K\bar{M}/M_0$, assuming $M_0 \gg 1$

$$\eta = \sqrt{\frac{K^2 - h^4}{K^2(K^2 - 1)h^2}} - h/K. \quad (20)$$

Note that η is only function of h and K . For example, if $h = 0.825$ (i.e., 17.5% antenna saving) and $K = 2$, then $\eta = 0.25$. This verifies Proposition 1, and we will verify it through numerical results in the next section. ■

IV. NUMERICAL RESULTS

This section presents numerical results that validate the theoretical radial- and transverse-velocity CRBs for the modular linear array. The carrier frequency is fixed at 28 GHz, while the system bandwidth and the CPI are set to $B = 100$ kHz and 2 ms, respectively. This corresponds to a pulse width of $T_s = 10^{-5}$ s and a total of $N = 200$ symbols per CPI. In addition, we set $G_t = G_r = 1$ and $\sigma_{RCS} = -23$ dB. The noise density power is set to -174 dBm/Hz and the transmit power $P_t = -10$ dBm.

Fig. 2 shows the array-gain reduction due to velocity estimation errors. More specifically, the minimum (i.e., worst) value of $|\psi(n)|^2$ within a CPI is plotted against radial Δv_r and transverse Δv_t velocity mismatch. It is evident that transverse-velocity mismatch results in a much more pronounced array-gain reduction than radial-velocity mismatch. This increased sensitivity to Δv_t arises because the transverse velocity induces an element-dependent Doppler shift, which damage coherent combining across the array elements. Furthermore, the closed-form array gain expression in (9) closely matches the exact expression in (7).

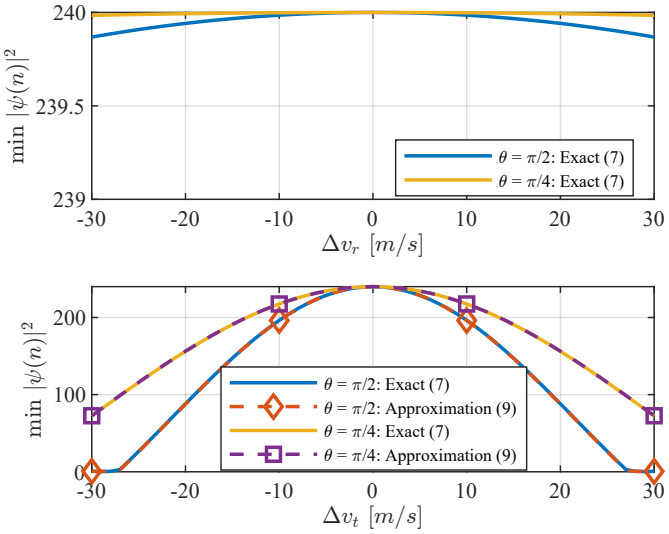


Fig. 2. Effect of velocity mismatch on the array gain when $r = d_F$ and $L = 61$.

The mean-squared error (MSE) of the MLE proposed in [1] is plotted in Fig. 3 and compared to the derived CRBs. The MSE is estimated via Monte Carlo simulation with 1000 iterations for each value. The ground-truth velocities are $v_r = 10$ m/s and $v_t = 8$ m/s. In addition, the MLE is initialized with the values (11, 7). Although this initialization is close to the ground-truth values, it is justified within the predictive beamforming framework [1]. It can be noted that the MSE matches the derived CRBs (16) and (17) for the case of single ULA. Overall, the estimation accuracy of v_r and v_t are substantially different. The transverse CRB is much larger than the radial CRB, because the transverse velocity contributes significantly less Fisher information. In addition, the transverse CRB of the MLA is lower than the MSE because of the increased aperture length, while for radial CRB there is no difference between the two cases.

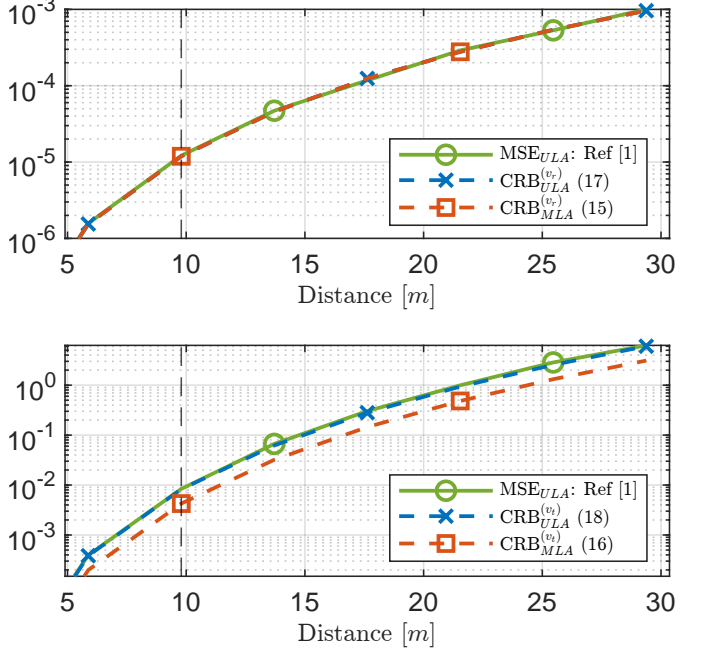


Fig. 3. The MSE of MLE in [1] and the derived CRBs. The total number of antenna used is 240. For the modular array, the number of modules is 2, the number of antennas in each module is $M = 120$, and the modular spacing parameter $L = 61$.

To understand the interplay between array geometry and estimation accuracy, Fig. 4 presents the radial and transverse CRBs for different array configurations without considering the effect of pathloss. The 240-element MLA achieve lower transverse CRB than collocated ULA while the radial CRB is not affected by the inter-module separation. In addition, the first 198-element MLA design (solid, $\bar{L} = 61$, $K = 2$, and $\bar{M} = 99$) matches the 240-element collocated ULA's transverse-velocity CRB while using about 17.5% fewer elements. However, the reduction in the number of antenna costs about 1.6 dB increase in the radial CRB, which is relatively negligible. The second 198-element MLA design (dashed, $\bar{L} = 103$, $K = 2$, and $\bar{M} = 99$) has wider inter-module spacing to attain the same aperture as the 240-element MLA but with less number of antennas yet, the radial CRB is not affected. These comparisons confirm that enlarging inter-module separation reduces the transverse-velocity CRB through effective-aperture growth, whereas the radial-velocity CRB is largely insensitive to separation because the dependence enters only via the small squared ratio $(\delta/r)^2$ in (14).

V. CONCLUSION

In this paper, we have derived the CRBs for joint radial and transverse velocity estimation with MLAs in the NF regime and established a closed-form characterization of the array gain under velocity mismatch, revealing that inaccurate transverse-velocity estimation can severely degrade the beamforming gain. Our results also show that increasing the inter-module separation enlarges the effective aperture and reduces the transverse-velocity CRB, whereas the radial-velocity CRB is largely insensitive to this separation. Moreover, we demon-

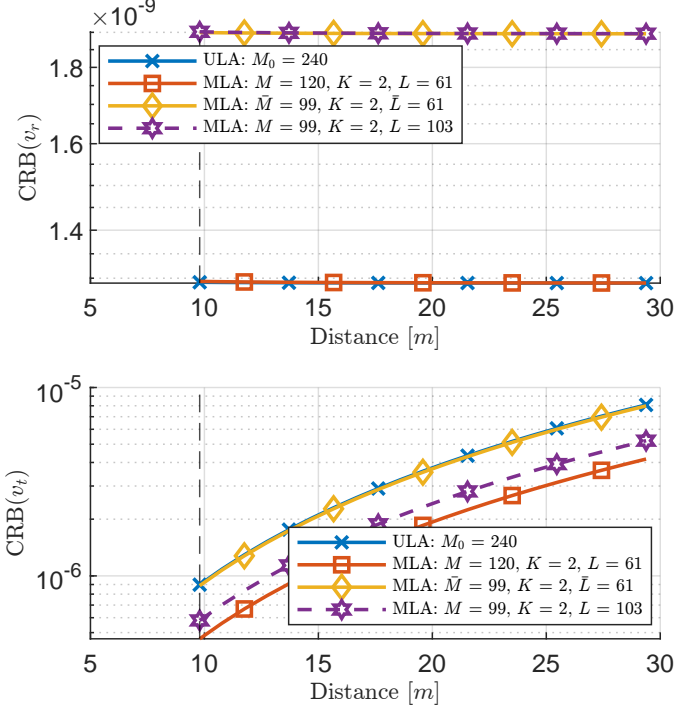


Fig. 4. CRB for radial velocity (top) and transverse velocity (bottom), with $\theta = \pi/2$. The gray dashed line indicates the Fresnel distance of the MLA with $M = 120$ and $L = 61$.

strate that, with an inter-module separation corresponding to 25% of a ULA aperture, an MLA with approximately 17% fewer antennas can attain the same transverse-velocity CRB as a collocated ULA while incurring a negligible loss in radial-velocity accuracy. This tradeoff is justified by the fact that the radial-velocity CRB is much lower than its transverse counterpart. Future work could include adopting an extended-target model instead of a point-like target, as well as investigating velocity estimation in multi-target scenarios.

APPENDIX

PROOF OF THEOREM 1

To simplify the summation, $g = Uk + m$ where $\epsilon = \delta/r$,

$$p_{m,k}^2 = \frac{(g\epsilon \sin \theta)^2}{1 - 2(g\epsilon) \cos \theta + (g\epsilon)^2}. \quad (21)$$

Set $x = g\epsilon$ and define the function $f(x) \triangleq \frac{x^2 \sin^2 \theta}{1 - 2x \cos \theta + x^2}$. Observe that, $x \in [-\bar{x}, \bar{x}]$, where the maximum value of x occurs at the edge of the array i.e., $\bar{x} = (U \frac{K-1}{2} + \frac{M-1}{2}) \epsilon$. Given that $\epsilon \ll 1$ and its maximum value occurs at the Fresnel distance when $\epsilon = \delta/d_F$, then

$$\max\{|\bar{x}|\} = \sqrt{\frac{\lambda/\delta}{U(K-1) + (M-1)}}, \quad (22)$$

the quantity $|\bar{x}|$ can be made arbitrary small if and only if $U(K-1) + M-1 \gg \lambda/\delta$. Then using Taylor series expansion around $x = 0$, one can approximate $f(x) \approx x^2 \sin^2 \theta$. Since $p_{m,k}^2 = f(g\epsilon) \approx (\epsilon \sin \theta)^2 g^2$, then the summation becomes

$$\begin{aligned} \sum_{m,k} p_{m,k}^2 &\approx (\epsilon \sin \theta)^2 \sum_{m,k} (Uk + m)^2, \\ &= (\epsilon \sin \theta)^2 \sum_k \sum_m (U^2 k^2 + 2Ukm + m^2), \\ &= \frac{MK}{12} (U^2(K^2 - 1) + M^2 - 1) \epsilon^2 \sin^2 \theta. \end{aligned} \quad (23)$$

Similarly, using Taylor expansion, one can approximate the off-diagonal term as

$$\begin{aligned} q_{m,k} p_{m,k} &= \frac{g\epsilon \sin \theta (1 - g\epsilon \cos \theta)}{1 - 2(g\epsilon) \cos \theta + (g\epsilon)^2}, \\ &\approx g\epsilon + (g\epsilon)^2 \sin \theta \cos \theta, \end{aligned}$$

Note that, due to symmetry, $\sum_{m,k} g = \sum_{m,k} Uk + m = 0$, hence the summation becomes

$$\sum_{m,k} q_{m,k} p_{m,k} \approx \frac{MK}{12} (U^2(K^2 - 1) + M^2 - 1) \epsilon^2 \sin \theta \cos \theta, \quad (24)$$

Therefore, the proof of Theorem 1 is completed.

REFERENCES

- [1] Z. Wang, X. Mu, and Y. Liu, "Near-field velocity sensing and predictive beamforming," *IEEE Transactions on Vehicular Technology*, 2024.
- [2] C. Giovannetti, N. Decarli, and D. Dardari, "Performance bounds for velocity estimation with extremely large aperture arrays," *IEEE Wireless Communications Letters*, vol. 13, no. 12, pp. 3513–3517, 2024.
- [3] A. Kosasih, Ö. T. Demir, and E. Björnson, "Achieving beamfocusing via two separated uniform linear arrays," in *2024 58th Asilomar Conference on Signals, Systems, and Computers*, 2024, pp. 168–172.
- [4] W.-C. Kao, J.-Y. Wu, S.-H. Tsai, and T.-Y. Wang, "Fast ambiguity-free subspace-based multiple aoa estimation for hybrid linear arrays," in *2023 IEEE 34th Annual International Symposium on Personal, Indoor and Mobile Radio Communications (PIMRC)*, 2023, pp. 1–5.
- [5] X. Li, Z. Dong, Y. Zeng, S. Jin, and R. Zhang, "Multi-user modular xl-mimo communications: Near-field beam focusing pattern and user grouping," *IEEE Transactions on Wireless Communications*, vol. 23, no. 10, pp. 13 766–13 781, 2024.
- [6] X. Li, H. Lu, Y. Zeng, S. Jin, and R. Zhang, "Near-field modeling and performance analysis of modular extremely large-scale array communications," *IEEE Communications Letters*, vol. 26, no. 7, pp. 1529–1533, 2022.
- [7] S. Yang, X. Chen, Y. Xiu, W. Lyu, Z. Zhang, and C. Yuen, "Performance bounds for near-field localization with widely-spaced multi-subarray mmwave/thz mimo," *IEEE Transactions on Wireless Communications*, vol. 23, no. 9, pp. 10 757–10 772, Sep. 2024.
- [8] C. Meng, D. Ma, X. Chen, Z. Feng, and Y. Liu, "Cramér–rao bounds for near-field sensing: A generic modular architecture," *IEEE Wireless Communications Letters*, vol. 13, no. 8, pp. 2205–2209, 2024.
- [9] A. Sabharwal, P. Schniter, D. Guo, D. W. Bliss, S. Rangarajan, and R. Wichman, "In-band full-duplex wireless: Challenges and opportunities," *IEEE Journal on Selected Areas in Communications*, vol. 32, no. 9, pp. 1637–1652, 2014.
- [10] Z. Wang, P. Ramezani, Y. Liu, and E. Björnson, "Near-field localization and sensing with large-aperture arrays: From signal modeling to processing," *IEEE Signal Processing Magazine*, vol. 42, no. 1, pp. 74–87, 2025.
- [11] Y. Liu, Z. Wang, J. Xu, C. Ouyang, X. Mu, and R. Schober, "Near-field communications: A tutorial review," *IEEE Open Journal of the Communications Society*, 2023.
- [12] A. Hussain, A. Abdallah, A. Celik, and A. M. Eltawil, "Joint motion, angle, and range estimation in near-field under array calibration imperfections," *arXiv preprint arXiv:2507.13463*, 2025.
- [13] K. M. Braun, "Ofdm radar algorithms in mobile communication networks," Ph.D. dissertation, Karlsruhe, Karlsruher Institut für Technologie (KIT), Diss., 2014, 2014.
- [14] S. M. Kay, *Fundamentals of statistical signal processing: estimation theory*. USA: Prentice-Hall, Inc., 1993.